NANO LETTERS

pubs.acs.org/NanoLett

Light-Induced Local Heating for Thermophoretic Manipulation of DNA in Polymer Micro- and Nanochannels

Lasse H. Thamdrup, Niels B. Larsen, and Anders Kristensen*

Department of Micro- and Nanotechnology, Technical University of Denmark, DK-2800 Lyngby, Denmark

ABSTRACT We present a method for making polymer chips with a narrow-band near-infrared absorber layer that enables light-induced local heating of liquids inside fluidic micro- and nanochannels fabricated by thermal imprint in polymethyl methacrylate. We have characterized the resulting liquid temperature profiles in microchannels using the temperature dependent fluorescence of the complex $[Ru(bpy)_3]^{2+}$. We demonstrate thermophoretic manipulation of individual YOYO-1 stained T4 DNA molecules inside micro- and nanochannels.

KEYWORDS Lab-on-a-chip, opto-thermal actuation, thermophoresis

Over the past decade, nanofluidic structures have emerged as a highly versatile and useful platform for studying genomic-length DNA. Prominent examples include real-time investigation of the interaction sites of restriction enzymes[1] and repressor proteins[2] in straight nanochannels, confinement spectroscopy of small conformational changes in tapered nanochannels,[3] entropically induced filtering of multidisperse samples in slitlike structures with periodically alternating depths[4] and probeless immobilization and self-organization of single molecules in slits with arrays of embedded pits.[5] Conventionally, DNA is transported inside micro- and nanofluidic structures by pressure-driven liquid flows or electrophoresis. However, these bulk-type methods of sample transport do not allow for manipulation of individual biomolecules. This possibility is offered by thermophoresis, which refers to the drift of particles or molecules along temperature gradients,[6] provided that highly localized liquid temperature gradients can be established and controlled in a flexible manner. Several possibilities exist for local heating of liquids inside polymer fluidic structures. The temperature of liquids may be controlled by Joule heating by implementing, for example, metal electrodes[7] or utilizing electrokinetic pumping.[8] However, these methods are best suited for applications that only require increased liquid temperature at well-defined locations. Heating, based on the infrared absorption of water in microscale structures,[9,10] provides a highly flexible way of increasing the temperature locally. Nevertheless, this technique demands high laser intensity (~1 W, laser spot size ~10 μm) and poses strict requirements on the illumination wavelength (i.e., $\lambda > 1000$ nm), which prohibits the use of, for example, low-cost laser diodes. By adding photothermal gold nanoparticles to the liquid, Liu et al.[11] demonstrated the ability to drive and guide liquid flow inside polydimethylsiloxane (PDMS) microchannels using a 20 mW laser at 785 nm with a spot size of approximately 10 μm. This technique is effective for local heating near liquid−air interfaces but it is inapplicable for continuous bulk liquid heating in micro- and nanochannels and furthermore the presence of nanoparticles may influence the biological samples, such as DNA, being investigated. Recently, Boyd et al.[12] demonstrated local heating near liquid−air interfaces inside microfluidic channels by illuminating gold nanoparticle arrays at the plasmon resonant frequency using a 532 nm laser with a spot size of ~10 μm. The applicability of this technique is hampered by its inability to increase the temperature of bulk liquid volumes. Another approach has been presented by Krishnan et al.[13] where light from a low-power 405 nm laser with a spot size of ~10 μm is absorbed and converted into heat in thin films of gold and indium tin oxide. Although this technique allows for heating liquids in microchannels above 35 °C, it is incompatible with the fabrication of cheap all-polymer devices. Furthermore, as most polymer materials used for making lab-on-a-chip applications (e.g., polymethyl methacrylate (PMMA), PDMS, polycarbonate, and cyclic olefin copolymers as Topas) exhibit high autofluorescence under near-UV illumination,[14,15] fluorescence measurements on single biomolecules (e.g., genomic-length DNA) being manipulated by thermophoresis in nanoscale confinements may be troublesome or even impossible.

Here we present a fabrication scheme for making polymer chips that enable light-induced local heating (LILH) of liquids inside micro- and nanofluidic channels using light from a near-infrared laser diode (maximum laser power of 42 mW, minimum $1/e^2$ spot width of 5 μm and peak

* To whom correspondence should be addressed- E-mail: anders.kristensen@nanotech.dtu.dk.

Received for review: 09/27/2009
Published on Web: 02/18/2010

DOI: 10.1021/nl903190q | *Nano Lett.* **2010,** *10,* 826–832

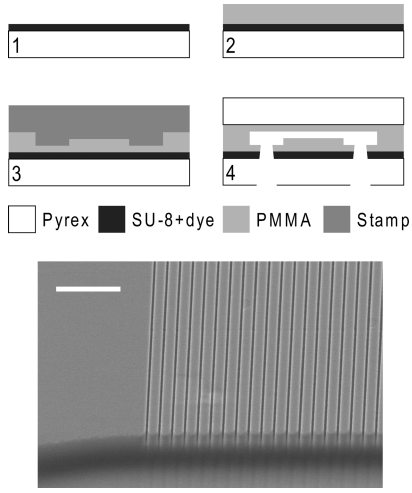

FIGURE 1. (Top) The fabrication process. (1) Deposition of absorber layer, (2) spin coating PMMA thin film, (3) thermal imprint with two-level hybrid stamp, (4) powder blasting of liquid access holes and sealing by thermal polymer−polymer bonding. (Bottom) Scanning electron microscopy image of an imprint showing the array of nanochannels interfacing one of the microchannels. The scale bar is 5 μm. Prior to imaging, 10 nm Al was deposited.

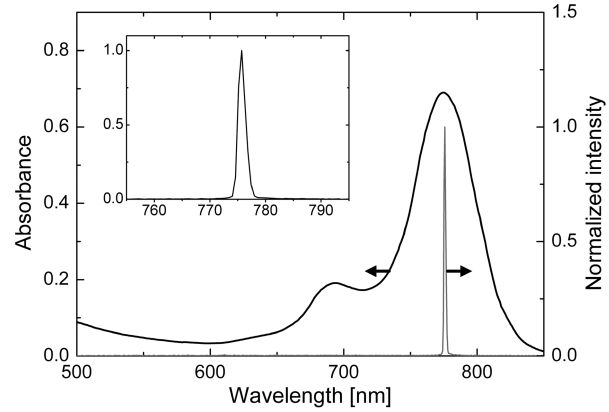

FIGURE 2. Absorbance of SU-8 with PROJET 800NP. The gray line indicates the spectrum of the utilized laser diode which has a peak emission at 775 nm. The inset is a magnified view of the laser emission spectrum.

emission wavelength of 775 nm). The use of a near-infrared source for heating circumvents problems of polymer autofluorescence observed for shorter wavelength illumination. Light-to-heat conversion occurs in a 500 nm thick layer consisting of the epoxy-based negative resist SU-8 containing a phthalocyanine dye that absorbs strongly at 775 nm. By focusing light into the absorber layer, heat is generated by energy conversion and rapidly conducted through a thin residual polymer layer into the liquid. We have used the linear temperature dependence of the fluorescence of $[Ru(bpy)_3]^{2+}$ dissolved in Milli-Q water to characterize the temperature profiles in 50 μm wide and 900 nm deep fluidic channels. Furthermore, we show that single genomic-length T4 DNA molecules may be manipulated by thermophoresis inside the aforementioned microchannels as well as inside nanochannels having a height and width of 250 nm.

Fabrication. The first step in the fabrication scheme for producing the polymer chips (Figure 1) is the deposition of a dedicated absorber layer. This layer consists of a commercially available phthalocyanine dye (PROJET 800NP, Fujifilm) dissolved in the epoxy-based negative resist SU-8 (SU-8 2002, Microchem Corp.). A solution containing 14.5 wt% SU-8 and 0.4 wt% dye dissolved in pure cyclopentanone was spin coated on a 500 μm thick 4 in. borosilicate glass wafer (Jinsol). After a pre-exposure bake at 90 °C for 2 min, the thin film was flood exposed (EVG Aligner AL6−2) using a dose of 1500 mJ/cm^2. Subsequently, a postexposure bake at 90 °C for 2 min was carried out before immersing the substrate in propylene glycol monomethyl ether acetate for 1 min followed by isopropanol rinsing and spin drying. The thin film-coated substrate was hereafter left on a hotplate at 150 °C for 20−30 min to increase the cross-linking density and substrate adhesion. The final thickness of the layer is approximately 500 nm as measured by stylus profilometry. The homogeneity of the dye distribution throughout the depth of the layer was investigated by X-ray photoelectron spectroscopy (XPS) measurements. As the phthalocyanine dye contains Cu,[16] we have used the atomic percentage of this element for verifying the vertical and lateral homogeneity of the dissolved dye in the SU-8 thin film on a 4 in. wafer. The homogeneity is an important prerequisite for ensuring consistency regarding the energy conversion properties and thereby the obtainable liquid temperatures inside the fluidic channels. The absorption spectrum of the energy conversion layer (Figure 2) exhibits a relatively narrow peak at approximately 775 nm. Before thermal imprint, a 1.2 μm thick low molecular weight PMMA film (PMMA 50k, Microchem Corp.) was spin coated on top of the absorber layer. The adhesion between PMMA and SU-8 is excellent,[17] which alleviates the need for an adhesion promoter. After spin coating, the solvent (anisole) was evaporated by baking the substrate on a hot plate at 150 °C for 10 min. Fluidic channels were transferred to the PMMA layer by thermal imprint (EVG 520 Hot Embosser) using a 4 in. two-level hybrid stamp.[18] The stamp allows for replicating two 50 μm wide and 900 nm deep channels bridged by an array of 200 nanochannels having a height and width of 250 nm (Figure 1). The imprint was performed using a piston force of 10 kN at a temperature of 190 °C for 15 min. After thermal imprint, the residual layer underneath the micro- and nanochannels is 300 nm and 1 μm, respectively. Liquid access holes were powder blasted through the glass wafer using a microetching tool (Microetcher II, Danville Engineering). Afterwards, a 4 in. borosilicate glass wafer (Jinsol) with a 300 nm thick PMMA layer (PMMA 50k, Microchem Corp.) was used to seal the fluidic channels by thermal polymer−polymer bonding at the glass transition temperature (T_g = 105 °C) using a piston force of 3 kN for 10 min.

Measurement Setup and Experimental Details. To heat up liquids inside the micro- and nanochannels, an experimental setup has been established. Light from a laser diode

DOI: 10.1021/nl903190q | *Nano Lett.* **2010,** *10,* 826–832

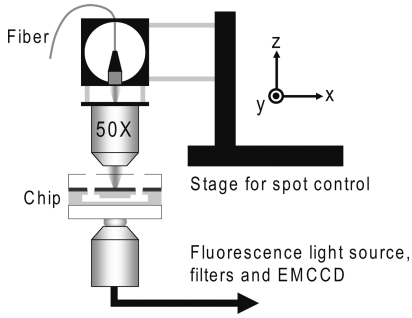

FIGURE 3. The experimental setup. Light from a laser diode is fiber launched and coupled into the absorber layer using a 50× NA 0.45 objective mounted on a *xyz*-stage for flexible control of spot size and position. Epi-fluorescence measurements were conducted on a modified Nikon microscope.

with a peak emission wavelength of 775 nm (Thorlabs) is fiber launched and focused into the absorber layer (Figure 3) using a 50× NA 0.45 objective (Leica). The current and temperature of the laser diode is controlled by a commercial mount and controller unit (Thorlabs) that enables reliable regulation of the emission spectrum and power (0−42 mW in the focal plane). The $1/e^2$ width of the focal spot was characterized using a knife-edge beam profiler (Melles-Griot) yielding a spot diameter of approximately 5 μm. The objective and fiber is mounted on a *xyz*-stage (Thorlabs) that provides micrometer precision in the control of the spot size and position. The laser light is introduced through the back of the chip. For all measurements, an inverted epi-fluorescence microscope (Nikon Eclipse TE2000-U) equipped with a metal halide fluorescence light source (Prior Lumen 200 W) and an EMCCD camera (CascadeII:512, Photometrics) was used. To filter out the relatively intense light from the laser source, an additional filter (transmission >95% for 390−690 nm, blocking optical density 6−8 for 730−1050 nm, Nikon) was inserted in a custom-made aluminum holder during all measurements. For the temperature measurements, a 30 mM solution of $[Ru(bpy)_3]^{2+}$ (Sigma-Aldrich) in Milli-Q water was used. As the ruthenium complex has a large Stokes shift, an unconventional filter combination (excitation, 465−495 nm; dichroic mirror, 505 nm; emission, 605−655 nm, Nikon) was used. Thermophoresis measurements on T4 DNA (166 kilo base pairs, Nippon Gene) stained with the bisintercalating cyanine dye YOYO-1 (Invitrogen) at a ratio of one dye molecule per five base pairs were conducted using a medium band B-2E/C filter combination (excitation, 465−495 nm; dichroic mirror, 505 nm; emission, 515−555 nm, Nikon). The DNA was suspended in a loading buffer consisting of 45 mM tris-base, 1 mM ethylenediaminetetraacetic acid (EDTA), 45 mM boric acid (i.e., 0.5× TBE) and 3 vol% β-mercaptoethanol to suppress bleaching of YOYO-1.[3,5] All solutions were degassed for 2 h before measurements.

Estimating the Temperature. Performing high-resolution real-time measurements of the local liquid temperature inside microfluidic channels is not a trivial task. As conventional fluorescent dyes such as rhodamine B and fluorescein exhibit a temperature-dependent fluorescence emission intensity,[19] they may be used for probing the local temperature in microfluidic channels by means of fluorescence microscopy. Recently, rhodamine B dissolved in aqueous solutions[20] or suspended in PDMS[21] has been used for such temperature measurements. However, the fluorescence intensity does not exhibit a linear temperature dependence which calls for thorough calibration schemes. The fluorescence intensity of the ruthenium complex $[Ru(bpy)_3]^{2+}$ has been shown to exhibit a high degree of linearity in the range 20−60 °C[22,23] and therefore represents an excellent probe. The high linearity enables a simple two point calibration scheme. For the calibration measurements, a cartridge heater with an embedded K-type thermocouple was used to heat a 30 mM $[Ru(bpy)_3]^{2+}$ solution inside the fluidic channels. The fluorescence intensity was measured in the microchannels at $T = 30$ and 50 °C and the intensity was seen to decrease by ∼2% per degree (the accuracy of the determined temperatures is ±1 °C). This value may be used for estimating the steady-state temperature profiles when conducting LILH. Four image stacks with 50 frames (exposure time of 100 ms) were acquired and averaged. Initially two stacks of the background, with and without the laser spot, were acquired. Hereafter, two stacks of the fluorescence with and without heating were acquired. The temperature in each pixel was subsequently calculated using eq 1

$$T = \mathrm{RT} + \frac{1}{0.02}\left(1 - \frac{I_{\mathrm{spot}}}{I_{\mathrm{illum}}}\right) \qquad (1)$$

where RT is the room temperature and I_{spot} and I_{illum} are the background corrected pixel intensities with and without heating. All temperature measurements were conducted with a 20× objective (Nikon) and a 1.5× lens (Nikon) fitted prior to the EMCCD. This gives a maximum spatial resolution of ∼0.5 μm. As seen from Figure 4, it is possible to heat the liquid to approximately 41 °C using a laser power of 38 mW. Since the heating is very local, steep temperature gradients of 1.5−2 °C/μm can be obtained near the center of the hot zone. By varying the laser power it is possible to adjust the maximum temperature increase and the local gradient environment to accommodate specific requirements (Figure 4). The thermal diffusivity of water[24] is approximately 1.4×10^{-7} m^2/s which yields a characteristic time for thermal diffusion over a length of 100 μm of $\tau \sim 100$ ms. Thus, the temperature profile may, for all practical reasons, be assumed to be in a steady state within no more than 1 s.

Three straightforward possibilities exist for increasing the maximum obtainable temperature inside the fluidic channels: (i) Reducing the residual layer thickness thereby facilitating heat transfer into the liquid, (ii) increasing the PMMA thickness on the bonding substrate, which will suppress heat transfer through the lid due to the lower thermal conductivity

DOI: 10.1021/nl903190q | *Nano Lett.* **2010,** *10,* 826–832

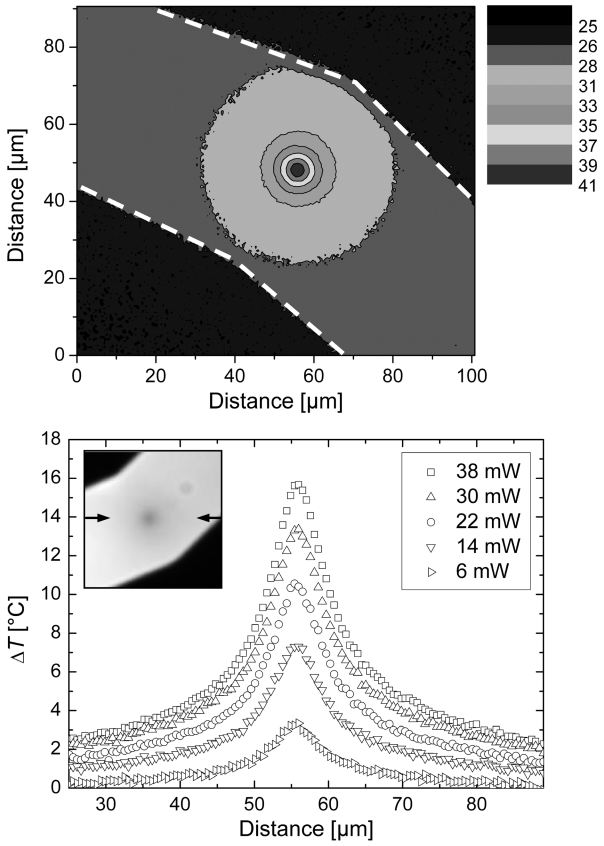

FIGURE 4. (Top) Contour plot showing the temperature inside the microfluidic channel when using a laser power of 38 mW. The room temperature was 25 °C. Only values inside the channel, outlined by dashed lines, have any physical significance. The temperature in each pixel was calculated according to eq 1 and the procedure outlined in the text. (Bottom) Graph showing the increase in temperature, ΔT, across the microchannel for different values of the laser power. The room temperature was 25 °C. The inset shows an averaged fluorescence image with heating and the arrows indicate the direction along which the temperature profiles have been sampled. The full width at half-maximum (fwhm) of the heated zones is ~8 μm.

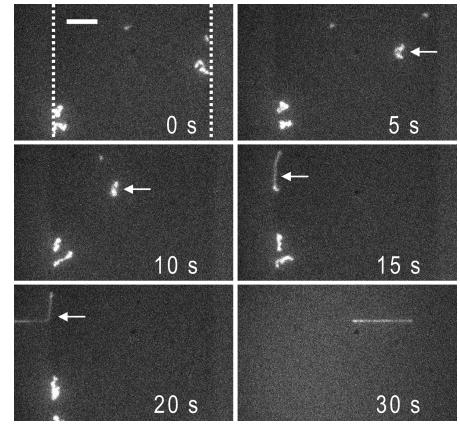

FIGURE 5. Series of fluorescence images showing thermophoretic manipulation of a single T4 DNA molecule. The white dotted line in the first image indicates the boundaries of the microchannel. The laser spot size is 10−15 μm and a power of 35 mW was used. The DNA is moved across the 50 μm wide microchannel and inserted into a 250 × 250 nm nanochannel by applying a slight pressure. The scale bar is 10 μm and the white arrows indicate the approximate position of the spot center. The field-of-view is shifted to the left at $t = 30$ s where the DNA is confined in the nanochannel.

of PMMA as compared to water (i.e., $k_{PMMA} = 0.19$ W/m · K[25] and $k_{water} = 0.61$ W/m · K[26]), and (iii) increasing the wt % of the phthalocyanine dye in the absorber layer to enhance the energy conversion.

Thermophoretic Manipulation of DNA. Thermophoresis is basically the migration of particles or molecules along temperature gradients (for a recent topical review article refer to ref 27). This mode of transport has received a growing interest in the field of microfluidics. Examples of recent applications include particle separation in silicon-based chips,[28] trapping of DNA by combined thermophoretic depletion and convection in PDMS chambers,[29] replication of DNA in convection cells by the polymerase chain reaction,[30] DNA extension in microscale glass cells,[31] and DNA accumulation by superposition of fluid flow and thermophoretic migration.[32] Furthermore, measurements on nanoscale polymer beads,[33,34] oil-in-water microemulsion droplets,[35] micellar solutions of, for example, sodium dodecyl sulfate,[36] proteins,[37] and DNA[38] have been conducted to investigate the subtle influence of particle size, charge and conformation on the thermophoretic mobility (also commonly termed the thermodiffusion coefficient) D_T that also depends on the buffer chemistry and temperature as well as the explicit concentration of the species being investigated.

Here we demonstrate thermophoretic manipulation of single genomic-length DNA molecules inside both micro- and nanochannels. Because of the small height of the channels (900 and 250 nm, respectively) heat and mass transfer due to convection will be negligible. Maximum temperatures during thermophoretic manipulation of DNA are measured to be below 40 °C as the spot was defocused (i.e., spot diameter of 10−15 μm) during manipulations. As seen in Figure 5, a single T4 DNA molecule can be moved across the 50 μm wide channel and inserted into a nanochannel using a slight pressure. The height, h, of the microchannel is actually slightly smaller than the bulk solution radius of gyration, R_g, which for a self-avoiding semiflexible polymer, such as DNA, is given by $R_g \approx (Pwr_{con}^3)^{1/5}$, where P and w are the persistence length and width (i.e., approximately 60 and 2 nm, respectively) and r_{con} is the contour length (i.e., the number of base pairs multiplied by the base pair spacing of 0.34 nm).[39] Using the stated numbers, $R_g \approx 1.8$ μm, which is in good agreement with an experimentally determined value of approximately 1.5 μm.[40] Since $h < R_g$, the DNA conformation as well as physical parameters such as the diffusivity, D, and thermophoretic mobility, D_T, are expected to differ slightly from what is observed in bulk solution. LILH starts at $t = 0$ s and within 15 s the DNA has been translated across the 50 μm wide channel

DOI: 10.1021/nl903190q | Nano Lett. 2010, 10, 826–832

yielding an average velocity of $v_{av} = 3.3\ \mu$m/s. Hence it is evident that thermophoresis is not an attractive technique for transporting samples over large distances. Instead, conventional sample transport techniques such as hydrodynamic pumping or electrophoresis should be used. However, thermophoresis by LILH allows for a very local and flexible manipulation of species. To estimate the thermophoretic force associated with LILH in the microchannel, we assume that $f_{th} \approx 6\pi\eta R_g v_{av}$, which yields $f_{th} \sim 100$ fN when substituting $R_g = 1.5\ \mu$m and the viscosity $\eta = 1.1$ mPa·s[40] as well as the determined value for v_{av}. Optical trapping of T4 DNA has been demonstrated in aqueous solutions containing polyethylene glycol using a highly divergent and intense laser source (i.e., laser power of 500 mW, spot size of 1 μm and NA of 1.3).[41] To address the influence of tweezer forces, we conducted reference measurements using chips without absorber layer and no influence of the LILH light source on DNA conformation could be discerned.

At $t = 15$ s (Figure 5) the DNA reaches the interface to the array of nanochannels. This interface represents an entropic barrier, as the DNA has to be stretched in order to enter a nanochannel. In mathematical terms, the total entropy of the DNA $S_{tot} = r_{con,m}s_m + r_{con,n}s_n$ where $r_{con,m}$ and $r_{con,n}$ is the DNA length stored in the micro- and nanochannel respectively with characteristic entropies per unit length given by s_m and s_n.[42] Since the entropy is proportional to ln Ω, where Ω is the number of available conformations, it is evident that DNA entrance into a nanochannel will be accompanied by a decrease in S_{tot} as the number of available DNA conformations is smaller in the nanochannel as compared to the microchannel (i.e., $s_n < s_m$). Therefore, an external force, with a magnitude comparable to the entropic recoil force, f_r, has to be applied in order to overcome the barrier.

As shown in refs 42 and 43, f_r may be estimated by performing measurements on the entropy driven recoil of DNA from low to high entropy regions. Therefore, we have performed measurements on DNA recoiling from the nanofluidic channels as seen in Figure 6. The insertion length, L_n, of DNA recoiling from a nanochannel is well approximated by

$$L_n = \sqrt{-\frac{f_r}{\rho}(t - t_0)} \tag{2}$$

where ρ is the hydrodynamic drag per unit length extended in the nanochannel and t_0 is the time where the DNA is completely extracted from the nanochannel.[42,43] The value of f_r/ρ is highly dependent on the system in consideration. For our particular system, a characteristic ratio between the recoil force and drag coefficient of $22.7 \pm 2.1\ \mu$m^2/s was measured. This value is approximately a factor 3 higher than the value reported in ref 43, where DNA recoils from 90 nm wide and 100 nm high nanochannels (yielding a geometric average of $d = 95$ nm) into a micrometer wide nanoslit with $h = 100$ nm. The most probable explanation for this discrepancy is that as the microchannels in our device has $h \sim R_g$, the DNA essentially escapes into an environment bearing close resemblance to bulk solution. This will increase the number of available conformations in the microchannel and therefore also the entropy. As f_r is the direct result of an abrupt entropy increase, this will lead to higher recoil forces. To arrive at an order of magnitude value for f_r, we have used an analytical expression[44] for ρ in nanochannels in the de Gennes regime (i.e., $d \gg P$)

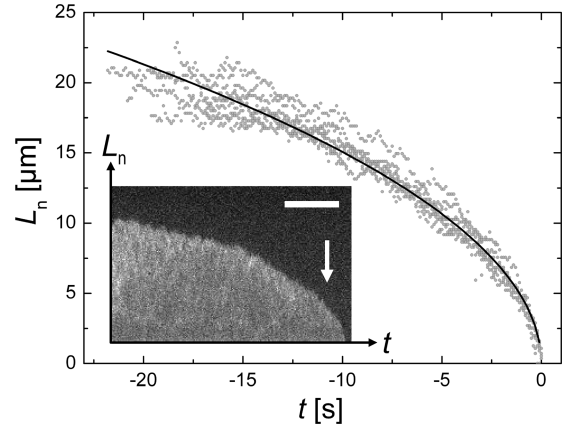

FIGURE 6. Graph showing the DNA insertion length, L_n, in the nanochannel versus time for eight different T4 DNA molecules undergoing entropic recoil into the microchannel. The data has been shifted so that $t_0 = 0$ s for all eight recoil events. The black line is a fit to the average of the data points using eq 2 with $f_r/\rho = 22.7 \pm 2.1$ μm^2/s. The inset shows stacked fluorescence micrographs (i.e., a timetrace) of a T4 DNA molecule (bright region) undergoing entropic recoil. The scale bar is 10 μm and the arrow indicates the direction of f_r. The DNA recoils into the microchannel within 21 s.

$$\rho = 6\pi\eta\frac{(Pw)^{1/3}}{d^{2/3}} \tag{3}$$

which gives $\rho \sim 3$ fN·s/μm^2. This value allows us to estimate $f_r \sim 50$ fN. As the entropic recoil force is comparable to the thermophoretic force, selective introduction of single DNA molecules into the nanochannels solely by LILH is feasible. When the DNA reaches the interface to the array of nanochannels at $t = 15$ s (Figure 5) it is stretched. The stretching against the channel array greatly increases the possibility of an event where a part of the contour is seeded into a nanochannel.[45] The entrance is facilitated by applying a slight pressure. Therefore, thermophoretic manipulation by LILH makes it possible to selectively insert single DNA molecules into nanofluidic structures.

The obtainable temperature gradients associated with LILH also allows for deterministic manipulation of DNA in nanofluidic channels which the preliminary results, shown in Figure 7, clearly illustrate. In this case, the nanofluidic

DOI: 10.1021/nl903190q | *Nano Lett.* **2010,** *10,* 826–832

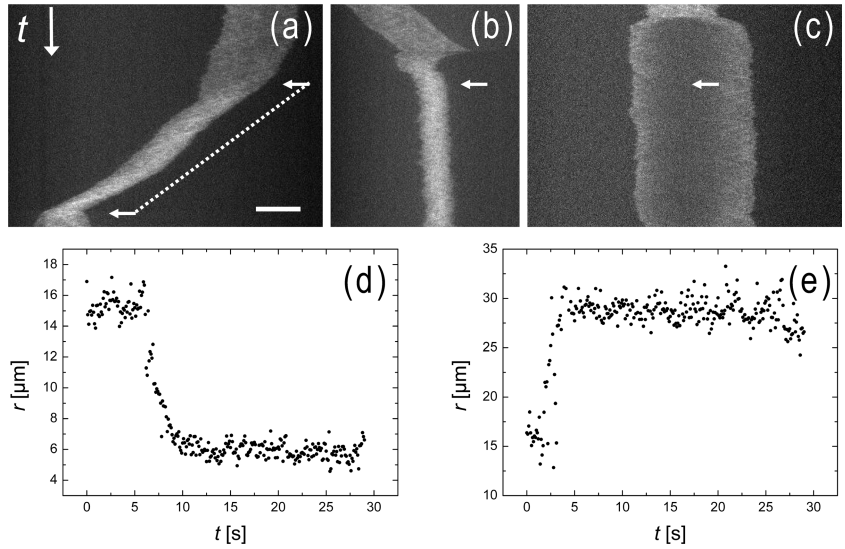

FIGURE 7. (a) Intensity time trace showing thermophoretic translation of T4 DNA inside a nanochannel using a laser power of 38 mW. The DNA is translated at 2.3 μm/s and the extension is reduced from 17.2 $\pm$ 1.0 μm to 9.1 $\pm$ 1.0 μm due to the balance between the imposed localized thermophoretic force and the hydrodynamic drag force. (b) Intensity time trace showing compressed T4 DNA inside a nanochannel. The DNA is compressed against the temperature gradient arising from LILH (laser power of 42 mW) using a slight pressure (~100 mbar). (c) Intensity time trace showing enhanced stretching of T4 DNA in a nanochannel by thermophoresis using a laser power of 30 mW. As the DNA is stretched due to the temperature gradient, the monomer density decreases which results in a low fluorescence signal in the stretched region. (d) Graph showing the extension, *r*, versus time, *t*, of the T4 DNA fragment in (b). The average extension before and during compression is 15.3 $\pm$ 0.7 μm and 5.9 $\pm$ 0.5 μm, respectively. The DNA is compressed by a factor 2.6. (e) Graph showing the extension, *r*, versus time, *t*, of the T4 DNA in (c). The average extension before and during stretching is 18.2 $\pm$ 1.2 μm and 28.9 $\pm$ 1.3 μm respectively. The DNA extension is enhanced by a factor 1.6. The arrows indicate laser spot position and the scale bar is 10 μm. The time span of the measurements is 29 s. The laser was slightly defocused giving a spot size of 10 μm. Room temperature during measurements was 25 °C.

channels merely serve as a scaffold for linearizing and confining the DNA which, according to de Gennes theory,[46] has an extension given by eq 4

$$r \cong r_{\mathrm{con}}\left(\frac{wP}{d^2}\right)^{1/3} \tag{4}$$

where r is the DNA extension in a nanochannel and $d = 250$ nm is the height and width of the quadratic nanochannels. Furthermore, the spring constant k of the confined DNA may be calculated from

$$k = \frac{k_{\mathrm{B}}T}{\sigma^2} \approx \frac{15}{4}\frac{k_{\mathrm{B}}T}{r_{\mathrm{con}}}\left(\frac{1}{Pwd}\right)^{1/3} \tag{5}$$

where σ is the standard deviation in the measured extension of DNA confined inside nanochannels.[39] As $\sigma \sim 1$ μm (refer to Figure 7), we may estimate the spring constant for small extension fluctuations of the confined DNA $k \approx 5$ fN/μm (for a more rigorous treatment of the spring constant of DNA refer to ref 47). This value indicates that the thermophoretic force associated with LILH is sufficient to perturb the thermodynamically stable conformation of nanoconfined DNA on a micrometer range. As opposed to optical tweezing,[48] where particles are trapped in intense and strongly divergent electromagnetic fields, this technique is better characterized as thermal pushing or pulling where the liquid temperature gradients are created by laser illumination and energy conversion in the thin absorber layer. DNA confined in a nanochannel may be approximated by a biological small-scale spring, where the spring constant may be estimated from eq 5. Inherent to a spring is the ability of being compressed and stretched when subjected to forces. As seen from Figure 7b,c, this allows for compression and enhanced nonuniform extension (detailed results to be published elsewhere) of DNA without altering channel dimensions[3,49] or the chemistry of the buffer solution.[50] Furthermore, as seen from Figure 7a, thermophoresis allows for selectively translating single DNA molecules inside nanochannels without applying hydrodynamic pumping or electrical fields.

Conclusion. We have presented a simple and low-cost fabrication scheme for making glass-supported polymer chips with a thin narrow-band absorber layer consisting of PROJET 800NP dissolved in SU-8. The absorber layer allows for energy conversion which enables light-induced local heating of liquids inside micro- and nanofluidic channels defined by thermal imprint in low molecular weight PMMA. We have characterized the maximum obtainable temperature and the resulting gradients in 900 nm deep and 50 μm wide channels using the temperature dependent fluorescence of the ruthenium complex $[Ru(bpy)_3]^{2+}$. Furthermore, we have shown that the fabricated chips may be used for thermophoretic manipulation of genomic-length DNA. The

DOI: 10.1021/nl903190q | *Nano Lett.* **2010,** *10,* 826–832

steep temperature gradients associated with LILH allows for movement of DNA both inside micro- and nanochannels as well as compression or enhanced stretching of DNA in nanochannels. As the spring constant of nanoconfined DNA is in the femto-Newton regime, even small values of ∇T will allow for significant influence on the conformation of confined DNA. Our results clearly support the hypothesis that thermophoresis is a viable method for probing single biomolecules in nanoscale confinements. It may be used for stretching, for example, circular DNA in nanoslits or even stretching single-stranded DNA in smaller scaffold channels. Furthermore, LILH is an excellent technique for performing local entropy sculpting by localized heating.

Acknowledgment. This work was financially supported by the Danish Research Council for Technology and Production, FTP grant no. 274-050375. The partial support of the EC funded project READNA (Contract no. HEALTH-F4-2008-201418) is gratefully acknowledged.

REFERENCES AND NOTES

(1) Riehn, R.; Lu, M.; Wang, Y. M.; Lim, S. F.; Cox, E. C.; Austin, R. H. *Proc. Natl. Acad. Sci. U.S.A.* **2005**, *102*, 10012.
(2) Wang, Y. M.; Tegenfeldt, J. O.; Reisner, W.; Guan, X. J.; Guo, L.; Golding, I.; Cox, E. C.; Sturm, J.; Austin, R. H. *Proc. Natl. Acad. Sci. U.S.A.* **2005**, *102*, 9796.
(3) Persson, F.; Utko, P.; Reisner, W.; Larsen, N. B.; Kristensen, A. *Nano Lett.* **2009**, *9*, 1382.
(4) Han, J.; Craighead, H. G. *Science* **2009**, *288*, 1026.
(5) Reisner, W.; Larsen, N. B.; Flyvbjerg, H.; Tegenfeldt, J. O.; Kristensen, A. *Proc. Natl. Acad. Sci. U.S.A.* **2009**, *106*, 79.
(6) Piazza, R. *Soft Matter* **2009**, *4*, 1740.
(7) Liu, J.; Enzelberger, M.; Quake, S. *Electrophoresis* **2002**, *23*, 1531.
(8) Ross, D.; Gaitan, M.; Locascio, L. E. *Anal. Chem.* **2002**, *73*, 4117.
(9) Braun, D.; Goddard, N. L.; Libchaber, A. *Phys. Rev. Lett.* **2003**, *91*, 158103–1.
(10) Duhr, S.; Braun, D. *Proc. Natl. Acad. Sci. U.S.A.* **2006**, *103*, 19678.
(11) Liu, G. L.; Kim, J.; Lu, Y.; Lee, L. P. *Nat. Mater.* **2006**, *5*, 27.
(12) Boyd, D. A.; Adleman, J. R.; Goodwin, D. G.; Psaltis, D. *Anal. Chem.* **2008**, *80*, 2452.
(13) Krishnan, M.; Park, J.; Erickson, D. *Opt. Lett.* **2009**, *34*, 1976.
(14) Piruska, A.; Nikcevic, I.; Lee, S. H.; Ahn, C.; Heineman, W. R.; Limbach, P. A.; Seliskar, C. J. *Lab Chip* **2005**, *5*, 1348.
(15) Wabuyele, M. B.; Ford, S. M.; Stryjewski, W.; Barrow, J.; Soper, S. A. *Electrophoresis* **2001**, *22*, 3939.
(16) Noreña-Franco, L. E.; Kvasnik, F. *Analyst* **1996**, *121*, 1115.
(17) Bubendorfer, A.; Liu, X.; Ellis, A. V. *Smart Mater. Struct.* **2007**, *16*, 367.
(18) Thamdrup, L. H.; Klukowska, A.; Kristensen, A. *Nanotechnology* **2008**, *19*, 125301.
(19) Coppeta, J.; Rogers, C. *Exp. Fluids* **1998**, *25*, 1.
(20) Ross, D.; Gaitan, M.; Locascio, L. E. *Anal. Chem.* **2001**, *73*, 4117.
(21) Samy, R.; Glawdel, T.; Ren, C. L. *Anal. Chem.* **2008**, *80*, 369.
(22) Filevich, O.; Etchenique, R. *Anal. Chem.* **2006**, *78*, 7499.
(23) Jorge, P. A. S.; Maule, C.; Silva, A. J.; Benrashid, R.; Santos, J. L.; Farahi, F. *Anal. Chim. Acta* **2008**, *606*, 223.
(24) Bindhu, C. V.; Harilal, S. S.; Nampoori, V. P. N.; Vallabhan, C. P. G. *Opt. Eng.* **1998**, *37*, 2791.
(25) Assael, M. J.; Antoniadis, K. D.; Wu, J. *Int. J. Thermophys.* **2008**, *29*, 1257.
(26) Ramires, M. L. V.; Fareleira, J. M. N. A.; Nieto de Castro, C. A.; Dix, M.; Wakeham, W. A. *Int. J. Thermophys.* **1993**, *14*, 1119.
(27) Piazza, R.; Parola, A. *J. Phys.: Condens. Matter* **2008**, *20*, 153102.
(28) Geelhoed, P. F.; Lindken, R.; Westerweel, J. *Chem. Eng. Res. Des.* **2006**, *84*, 370.
(29) Braun, D.; Libchaber, A. *Phys. Rev. Lett.* **2002**, *89*, 188103–1.
(30) Braun, D.; Goddard, N. L.; Libchaber, A. *Phys. Rev. Lett.* **2003**, *91*, 158103–1.
(31) Ichikawa, M.; Ichikawa, H.; Yoshikawa, K.; Kimura, Y. *Phys. Rev. Lett.* **2007**, *99*, 148104.
(32) Duhr, S.; Braun, D. *Phys. Rev. Lett.* **2006**, *97*, No. 038103.
(33) Duhr, S.; Braun, D. *Phys. Rev. Lett.* **2006**, *96*, 168301.
(34) Putnam, S. A.; Cahill, D. G.; Wong, G. C. L. *Langmuir* **2007**, *23*, 9221.
(35) Vigolo, D.; Brambilla, G.; Piazza, R. *Phys. Rev. E* **2007**, *75*, No. 040401−1.
(36) Piazza, R.; Guarino, A. *Phys. Rev. Lett.* **2002**, *88*, 208302–1.
(37) Iacopini, S.; Piazza, R. *Europhys. Lett.* **2003**, *63*, 247.
(38) Duhr, S.; Arduini, S.; Braun, D. *Eur. Phys. J. E* **2004**, *15*, 277.
(39) Tegenfeldt, J.; Prinz, C.; Cao, H. *Proc. Natl. Acad. Sci. U.S.A.* **2004**, *101*, 10979.
(40) Balducci, A.; Mao, P.; Han, H.; Doyle, P. S. *Macromolecules* **2006**, *39*, 6273.
(41) Ichikawa, M.; Yoshikawa, K.; Matsuzawa, Y. *J. Phys. Soc. Jpn.* **2005**, *74*, 1958.
(42) Turner, S. W. P.; Cabodi, M.; Craighead, H. G. *Phys. Rev. Lett.* **2002**, *88*, 128103–1.
(43) Mannion, J. T.; Reccius, C. H.; Cross, J. D.; Craighead, H. G. *Biophys. J.* **2006**, *90*, 4538.
(44) Liu, H. R.; Lee, A. P. *Integrated Biochips for DNA Analysis*; Riehn, R., et al., Eds.; Landes Bioscience and Spriner Science+Business Media: New York, NY, 2007.
(45) Han, J.; Turner, S. W.; Craighead, H. G. *Phys. Rev. Lett.* **1999**, *83*, 1688.
(46) de Gennes, P. G. *Scaling Concepts in Polymer Physics*; Cornell University Press: Ithaca, 1979.
(47) Marko, J. F.; Siggia, E. D. *Macromolecules* **1995**, *28*, 8759.
(48) Bustamante, C.; Bryant, Z.; Smith, S. *Nature* **2003**, *421*, 423.
(49) Reisner, W.; Morton, K. J.; Riehn, R.; Wang, Y. M.; Yu, Z.; Rosen, M.; Sturm, J. C.; Chou, S. Y.; Frey, E.; Austin, R. *Phys. Rev. Lett.* **2005**, *94*, 196101.
(50) Reisner, W.; Beech, J.; Larsen, N.; Flyvbjerg, H.; Kristensen, A.; Tegenfeldt, J. *Phys. Rev. Lett.* **2007**, *99*, No. 058302.

DOI: 10.1021/nl903190q | *Nano Lett.* **2010,** *10,* 826–832